Comprehensive study on flame retardant polyesters from phosphorus additives

Khalifah A. Salmeia [1], Ali Gooneie [1], Pietro Simonetti, Rashid Nazir, Jean-Pierre Kaiser [2], Alexandra Rippl [2], Cordula Hirsch [2], Sandro Lehner, Patrick Rupper, Rudolf Hufenus, Sabyasachi Gaan [*]

Advanced Fibers, Empa Swiss Federal Laboratories for Materials Science and Technology, St. Gallen, Switzerland

ABSTRACT

In this work we have performed a comprehensive study on synthesis, processing, detailed material characterization and preliminary assessment of toxicity of relatively new flame retardant (FR) additives as a key for developing environmentally friendly fire safe polyesters. Two 9,10-dihydro-9-oxa-10-phosphaphenanthrene-10-oxide (DOPO) based FR additives were synthesized using principles of green chemistry and incorporated via thermal processing in high temperature polyesters such as polyethylene terephthalate (PET) and polybutylene terephthalate (PBT). The green synthesis strategies included (i) the use of N-chlorosuccinimide as a sustainable chlorinating agent for DOPO and (ii) a solvent and catalyst free microwave-assisted synthesis. Atomistic molecular dynamics (MD) simulations were employed in order to calculate the solubility parameters of these additives so as to estimate their compatibility in the polyesters. Detailed rheological measurements of the polyester/FR blends were carried out and the results indicated a clear difference in all three additives tested. Based on these analyses, 6H-dibenz[c,e][1,2] oxaphosphorin,6-[(1-oxido-2,6,7-trioxa-1-phosphabicyclo[2.2.2]oct-4-yl)methoxy]-, 6-oxide (DOPO-PEPA) exhibited the highest compatibility with both polyesters and their blends and showed the highest thermal-oxidative stability guaranteeing stable and steady processing at high temperatures. All polyester/FR formulations exhibited higher flame retardancy compared to the virgin polyesters in the small scale fire tests. The FR additives were evaluated for their potential toxicity using a well-established *in vitro* platform. Our results indicate no acute cytotoxic potential for all FRs analyzed in two different cell types (the human lung epithelial cell line A549 and macrophages derived from the monocytic cell line THP-1) and under the chosen experimental conditions.

1. Introduction

There is increasing demand for the development of environmental friendly fire safe materials which fulfill both ecological and commercial requirements. In addition, these materials need to be fully characterized for their physical and chemical properties and their ease of processability for eventual industrial exploitation. Like in case of other additives, it is important that a flame retardant (FR) additive do not interfere with steady melt processing in typical polymer extruders. Therefore, it is required that the melt properties of the polymer/FR blends do not change significantly during the processing. Most common polymers are not suitable for fire safe applications and are rendered flame retardant by incorporating an FR additive in the polymer bulk or via coating on the surface. Incorporating FR additive in the bulk via thermal processing is relatively simple, economical and more durable to environmental influences. The key to reducing waste and improving sustainability of functional materials is to develop additives via green chemistry strategy. There are 12 important principles involved in green chemistry, for example, the chemical should be non-toxic, toxic raw materials and solvents should be avoided, high atom economy and the use of renewable feedstock [1].

Some halogenated flame retardants are prohibited [2] due the concerns regarding their toxicity [3]. In the last decades the

* Corresponding author.
  E-mail address: sabyasachi.gaan@empa.ch (S. Gaan).
[1] These authors contributed equally.
[2] Particles-Biology Interactions, Empa Swiss Federal Laboratories for Materials Science and Technology, St. Gallen, Switzerland.

impetus has shifted to the development of environmentally friendly flame retardants (FRs). Among the many classes of FR additives, new phosphorus containing FRs [4—7] are considered potential replacements for the toxic FRs [3]. More recently some phosphorus based FRs have also come under scrutiny of various regulatory and environmental agencies. Some phosphorus based FRs have been found to be toxic and are currently being phased out or their usage restricted [8—12].

A variety of new phosphorus compounds as potential replacement for toxic FRs have been synthesized by many researchers [4—7], however, in most cases the toxicity data of these compounds are unknown. Furthermore, they often employ synthesis strategies which do not follow the principles of green chemistry as outlined earlier, for instance, in some work phosphorus FRs have been synthesized with toxic carbon tetrachloride as reagent [13—16]. Among the phosphorus based FRs, development of 9,10-dihydro-9-oxa-10-phosphaphenanthrene-10-oxide (DOPO) and its derivatives have gained much attention in the research and industrial community due to its efficient and versatile FR action. They have recently been reported to be harmless for aquatic organisms and human cells [17,18]. DOPO and its derivative 6,6′-(ethane-1,2-diylbis(azanediyl))bis(6H-dibenzo[c,e][1,2]oxaphosphinine-6-oxide) (EDA-DOPO) do not induce acute cytotoxicity in human lung epithelial cell as well as human macrophages. Furthermore, both FRs are not neurotoxic and do not exhibit an influence on neural crest cell migration, or on the integrity of human skin equivalents. Furthermore, the two compounds have no effect on algae growth or daphnia viability at concentrations $\leq 400\,\mu M$ [18] which is one of the tests required for REACH registration in Europe [19]. Another DOPO derivative 10-(2,5-dihydroxyphenyl)-9,10-dihydro-9-xa-10-phosphaphenanthrene-10-oxide (DOPO-HQ) has also been evaluated for its eco-toxicity and was found to have toxicity markedly lower than commercially prevalent phosphates [20].

In this work we have evaluated in detail two DOPO derivatives (Fig. 1) as potential FR additives to develop nontoxic flame retardant polyester based materials. The DOPO derivatives 6H-Dibenz [c,e][1,2]oxaphosphorin, 6-[(1-oxido-2,6,7-trioxa-1-phospha bicyclo[2.2.2]oct-4-yl)methoxy]-, 6-oxide (DOPO-PEPA), 3-(6-oxidodibenzo[c,e][1,2]oxaphosphinin-6-yl)propanamide (AAM-DOPO) were synthesized taking into consideration the principles of green chemistry and processed with polyethylene terephthalate (PET) and polybutylene terephthalate (PBT) to make FR films. In addition to the synthesized DOPO derivatives a commercial phosphorous based FR Aflammit PCO 960 was used in this study for comparison. This commercial additive is known to be suitable for polyester applications; however, there exist little information in the literature regarding its processability and FR efficacy. The initial choice of these additives for this work was based on their reported high thermal stability [15,21]. The compatibilities of the FRs with the polyesters were checked by means of atomistic molecular dynamics (MD) simulations of the solubility parameters of the components. Furthermore, rheological measurements were performed to assess the melt characteristics of different polyester/FR systems

at the processing temperatures. The FR films were further evaluated for flammability using small scale fire tests. The toxicological profile of the additives was assessed using a well-established battery of *in-vitro* test. With these detailed multi-dimensional analyses, we aim to draw a comprehensive picture of the benefits of using these relatively new additives in combination with polyesters to develop environment friendly fire safe polyesters.

2. Experimental section

9,10-dihydro-9-oxa-10-phosphaphenanthrene-10-oxide (DOPO) was purchased from Metadynea GmbH (Austria), all other chemicals for synthesis were purchased from Sigma Aldrich (Switzerland) and were used without further purification. Aflammit PCO 960 was purchased from Thor GmbH, Germany. 1-oxo-4-hydroxymethyl-2,6,7-trioxa-l-phosphabicyclo[2.2.2]octane (PEPA) was bought from Carbosynth Limited, United Kingdom. The base polymers polyethylene terephthalate (PET) and polybutylene terephthalate (PBT) were provided by Serge Ferrari Tersuisse AG (Emmenbrücke, Switzerland) and Sukano AG (Schindellegi, Switzerland) respectively.

2.1. Synthesis of DOPO derivatives

2.1.1. Synthesis of DOPO-PEPA
DOPO (5.0 g, 23.1 mmol) was charged in a three-neck round bottomed flask connected to a condenser and N_2 inlet. Dry Toluene (50 mL) was added under nitrogen, followed by the addition of N-Chlorosuccinimide (NCS) (3.40 g, 25.4 mmol) in small portions via side arm under N_2 at ambient temperature. After complete addition, the reaction mixture was stirred at ambient temperature overnight. The white precipitates were removed by filtration under N_2 using Schlenk frit. The solvent was removed under vacuum. The residue was re-dissolved in dichloromethane (50 mL) and transferred under N_2 to a dropping funnel and was slowly added to a mixture of 1-oxo-4-hydroxymethyl-2,6,7-trioxa-l-phosphabicyclo [2.2.2]octane (PEPA) (4.17 g, 23.1 mmol) and triethylamine (2.80 g, 27.8 mmol) in dichloromethane (100 mL) at ambient temperature. The reaction was again stirred overnight at ambient temperature. The solvent was then completely removed and ethanol (50 mL) was added while stirring, forming a white product. The product was then collected by filtration and washed with ethanol and dried in vacuum at 80 °C until constant weight (4.45 g, 50% yield). The NMR data fit well with the earlier published reports (Fig. S1 of the Supporting Information) [15].

2.1.2. Synthesis of AAM-DOPO
DOPO (5.40 g, 25 mmol,), acrylamide (355 mg, 50 mmol) were placed in a heavy-walled glass vials sealed with aluminum crimp caps fitted with a silicon septum. The glass tube (with an inner diameter of 3 cm and a volume 60 mL) containing the reaction mixtures was sealed with a lid and heated in the microwave oven for 2 h at 120 °C (50 Bar, 1200 W) under N_2 atmosphere. The reactions were performed in Synthwave Microwave Single Reaction

Aflammit PCO 960　　**AAM-DOPO**　　**DOPO-PEPA**
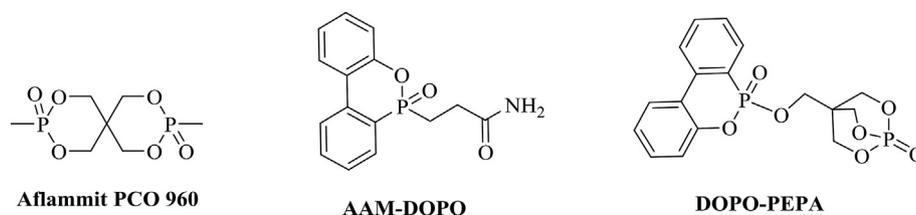
Fig. 1. General chemical structure of flame retardant additives.

Chamber provided by MWS Mikrowellen Systeme GmbH, Switzerland. The reaction mixture was continuously stirred with a magnetic stirrer during the irradiation. The temperature, pressure and irradiation power were monitored during the course of the reactions. After cooling down, the solids were washed with water and dried in vacuum at 80 °C as white powder with 66% yield. The NMR data (Fig. S2 of the Supporting Information) and the melting point concur well with the published data [21].

2.2. Atomistic simulations

Atomistic molecular dynamics (MD) simulations were employed in order to calculate the Hildebrand solubility parameters of different FRs used in this work [22]. In the simulations, the solubility parameters of different FRs were calculated from the cohesive energy of a system of molecules per unit of volume, i.e. the cohesive energy density (CED) [22,23]. Such a system of molecules was generated using the Amorphous Cell module of the BIOVIA Materials Studio [24] simulation software by including 50 molecules of each FR in a box and averaging over all configurations. The molecules in their full atomistic representations were allowed to interact with each other using the COMPASS force field provided in the Forcite module of the Materials Studio. Prior to CED calculations, the simulation box was allowed to equilibrate in a NPT ensemble for 500 ps to reach its equilibrium density at 400 K and 1 atm. It was checked that the systems reached their equilibrium densities in these simulations, see for example the equilibrated simulation box for DOPO-PEPA shown in Fig. 2. The solubility parameters were then calculated based on the various contributions of the force field interactions. The contributions of the van der Waals and electrostatic interactions to the total solubility parameter were also derived from the simulations.
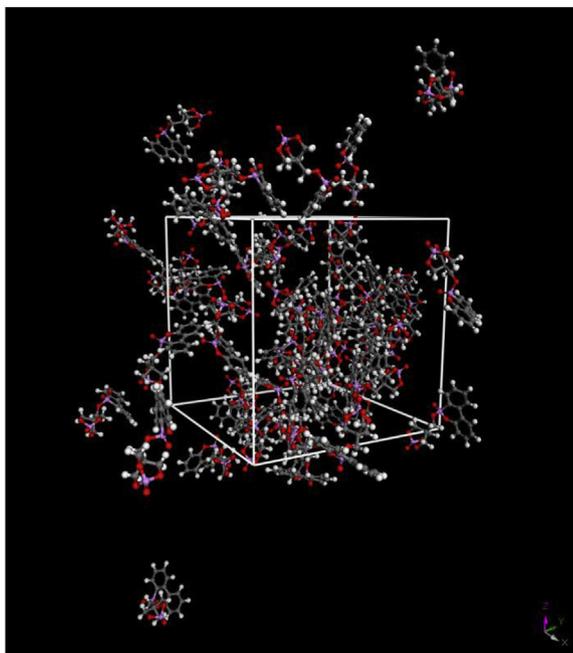
Fig. 2. The equilibrated simulation box after the MD simulations (the NPT run) containing atomistic representations of DOPO-PEPA molecules used to perform CED calculations. The colors represent different atoms as follows; white: H, red: O, purple: P, and gray: C. The simulation box has periodic boundary conditions on all sides. (For interpretation of the references to color in this figure legend, the reader is referred to the Web version of this article.)

2.3. PET film preparation

Polymers and FR additives were mixed with a gravimetric feeding system and subjected to a film extrusion line (Thermo Fisher Scientific, Karlsruhe, Germany) as depicted in Fig. 3. A Rheomex OS single screw extruder with diameter D = 19 mm and a length to diameter ratio of L/D = 25 was used to melt and feed the polymer to a Haake OS melt pump which in turn supplied the polymer melt at a fixed throughput to the slit die (width = 100 mm). A static mixer was installed between extruder and melt pump to improve the distributive mixing and temperature uniformity of the melt stream. The extruder pressure was set to 55 bar to ensure effective operation of the melt pump. Temperature of the calenders needed to solidify and shape the material was fixed at 65 °C, and the gap opening between the take-up calendars was set to 0.4 mm. Prior to extrusion, the polymers and the FR additives were vacuum dried for 12 h at 105 °C (PBT) and 125 °C (PET), respectively. Table 1 summarizes the various polyester/FR formulations and additional operating parameters of the different film extrusion trials performed in the present study are given in the Supporting Information (Table S1). Different concentration of flame retardant additives was taken in various formulations so as to keep the amount of phosphorus in the films constant. All manufactured films were around 0.5 mm thick and 60 mm wide. It should be noted that the control of additive content in the final films is a very sensitive process due to the intrinsic oscillations in the gravimetric feeding system. Thus it is likely that there will be small variations in final additive concentrations in various films. PBT and PET films were obtained as opaque and transparent material respectively and addition of the three additives had no significant influence on the films appearance.

2.4. Elemental analysis, thermal and fire characterization of the films

Phosphorus content analyses of the films was carried out using the inductively coupled plasma optical emission spectrometry method (ICP-OES), on an Optima 3000 (PerkinElmer AG, Rotkreuz, Switzerland) apparatus. Sample preparation for ICP-OES consisted of mixing 300 mg of sample with 1 mL H_2O_2 and 3 mL HNO_3, followed by digestion using a microwave.

Limiting Oxygen Index (LOI) values of all films were measured on FTT oxygen index apparatus according to ASTM D2863-97. The dimension of specimens for LOI test was 150×50 mm.

Vertical burning tests were performed according to the Swiss Standard (BKZ-VB) as described in the literature [25]. Polyester films in vertical orientation were exposed to a flame (45°) for 15 s and the burn length and burn time measured. Most thermoplastic fibers drip when exposed to fire and adequate heat. Thus in the
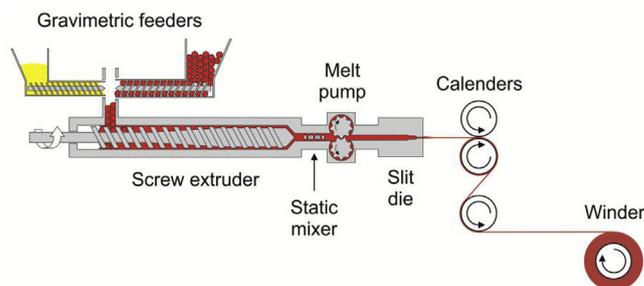
Fig. 3. Schematic assembly of the film extrusion line (The extruder pressure was set to 55 bar at the static mixture).

Table 1
Film formulations and basic extrusion parameters for polyester/FR blends.

Sample name	Base polymer	Additive/content [%]	Extrusion through-put [kg/h]	Extrusion temp. [°C]	Predicted phosphorus content [w%]	Measured phosphorus content [w%]
PBT	PBT	–	2.9	235	–	–
PBT/AF	PBT	3.0% Aflammit PCO 960	2.9	240	0.72	0.63
PBT/DP	PBT	5.0% DOPO-PEPA	2.9	235	0.78	0.77
PBT/AD	PBT	7.3% AAM-DOPO	2.8	235	0.79	0.53
PET	PET	–	2.8	270	–	–
PET/AF	PET	3.0% Aflammit PCO 960	2.8	270	0.72	0.64
PET/DP	PET	5.0% DOPO-PEPA	2.8	270	0.78	0.75
PET/AD	PET	7.0% AAM-DOPO	2.8	265	0.76	0.50

vertical burning tests the dripping behavior of the specimens was also observed. Five specimens were tested for LOI and vertical burning tests and an average value reported.

Direct insertion probe mass spectrometry (DIP-MS) was used to evaluate possible gas-phase activity and the degradation processes of the FRs. The samples were introduced into a quartz microcup in contact with a heating probe, whose tip was inserted into the ionization chamber, maintained at strongly reduced pressure of 10^{-6} mbar. DIP-MS analyses were conducted for $1-2\,\mu g$ polymer film samples using a ThermoQuest FINNIGAN instrument (Thermo Finnigan/Thermo Scientific, San Diego, CA, USA). The probe was heated from 50 to 450 °C at a rate of 10 °C/min.

Energy dispersive X-ray spectroscopy (EDX) was applied in combination with a scanning electron microscope (SEM) using an Inca X-sight device from Oxford Instruments (EDX) and a S-4800 microscope from Hitachi (SEM). For each sample, the EDX analysis was performed at two different areas on completely charred samples obtained from TGA, and an average value was obtained from the resulting elemental compositions. An area of about $100\,\mu m \times 100\,\mu m$ was scanned for the EDX measurements using an acceleration voltage of the electron beam of 20 kV, an emission current of $15\,\mu A$ and a working distance of 15 mm. Under these experimental conditions, the information depth is in the order of a couple of microns.

2.5. Rheological measurements

Rheological measurements were conducted on the extruded films of PBT and PET blends containing different FRs. Prior to the experiments, the samples were dried in a vacuum oven for 12 h at 100 °C and for 4 h at 140 °C to completely remove any moisture from the films before the tests. Two sets of tests were carried out on the samples utilizing an Anton Paar Physica 301 MCR rotational rheometer (Austria) equipped with a parallel plate fixture with a diameter of 25 mm and a constant gap of 1 mm. In the first set, oscillatory amplitude sweep tests were performed under a nitrogen environment at a constant oscillation frequency of 10 rad/s. In the second set, the thermal-oxidative stability of the melts were studied by measuring the evolution of oscillatory material functions at a constant oscillation frequency and strain of 1 rad/s and 1%, respectively, over 2 h under an oxygen environment. Before starting the measurements the samples were allowed to rest in the rheometer chamber for 30 s at the test temperature in order to reach a homogenous thermal equilibrium in the sample and minimize its prior history. Finally, it should be noted that all rheological tests on the PBT and PET samples were performed at constant temperatures of 250 and 290 °C, respectively.

2.6. In vitro toxicity assessment of FR additives

2.6.1. Flame retardant solutions

All FRs and some intermediates were solubilized in pure dimethylsulfoxid (DMSO) at a concentration of 500 mM. Serial predilutions were prepared in DMSO. Final dilutions were prepared in complete cell culture medium (MTS assay) or Hanks balanced salt solution (HBSS; DCF assay).

2.6.2. Cell culture conditions

The human alveolar epithelial cell line A549 (ATCC: CCL185) as well as the human mono-cytic cell line THP-1 (ATTC: TIB-202) were used to assess FR toxicity in vitro. Both cell lines were cultured in Roswell Park Memorial Institute (RPMI-1640) medium (Sigma-Aldrich) supplemented with 10% FCS (Fetal Calf Serum) (Lonza), 2 mM L-glutamine (Gibco), 50 μg/mL penicillin (Gibco), 50 μg/mL streptomycin (Gibco), and 100 μg/mL neomycin (Gibco) at 37 °C in a humidified atmosphere containing 5% CO_2 (hereafter referred to as complete cell culture medium and standard growth conditions, respectively). The adherently growing A549 cells were subcultured at approximately 80—90% confluency using 0.5% trypsin-EDTA (Sigma-Aldrich). In contrast THP-1 cells grew in suspension cultures and were subcultured by replacement of the medium when the cell density reached 8×10^5 cells/mL. Cell concentrations were not allowed to exceed 10^6 cells/mL. All experiments using THP-1 cells were carried out after differentiation of THP-1 monocytes into macrophages. Therefore cells were grown in the presence of 200 nM phorbol-12-myristate-13-acetate (PMA; Sigma-Aldrich) for 72 h.

2.6.3. Cell viability assessment (MTS assay)

A549 cells were seeded at a density of 1×10^4 cells per well of a 96-well cell culture plate in 200 μL complete cell culture medium and grown over night under standard growth conditions. Thereafter cells were treated for 48 h with 100 μL standard growth medium per well containing increasing concentrations of the FRs or the positive control agent $CdSO_4$. CellTiter96® AQueous One Solution (Promega) containing MTS (3-(4,5-dimethylthiazol-2-yl)-5-(3-carboxymethoxy-phenyl)-2-(4-sulfophenyl)-2H) as a water-soluble tetrazolium compound was used in accordance with the manufacturer's protocol. After 1 h of incubation under standard growth conditions absorption was detected at 490 nm using a Multimode plate reader (Mithras[2], Berthold Technologies).

THP-1 cells were seeded at a density of 8×10^4 per well of a 96-well cell culture plate in 200 μL complete cell culture medium containing 200 nM PMA and allowed to differentiate under standard growth conditions for 72 h. Thereafter cells were washed twice with pre-warmed (37 °C) phosphate buffered saline (PBS). Treatment and absorption measurement were carried out as described for A549 cells above.

2.6.4. Detection of reactive oxygen species (ROS) (DCF assay)

For the detection of ROS the dichlorofluorescein (DCF) assay (Molecular Probes) was used. A549 cells were seeded at a density of 2×10^4 cells per well of a 96-well cell culture plate in 200 µL complete cell culture medium and grown over night under standard growth conditions. The cells were then loaded with 2′,7′-dichlorodihydrofluorescein diacetate (H$_2$DCF-DA; 50 µM in HBSS) for 1 h under standard growth conditions. After two washing steps with pre-warmed (37 °C) HBSS cells were treated for 2 h with 100 µL HBSS per well containing increasing concentrations of flame retardants. The peroxynititrite-generating compound 3-morpholinosydnonimine (Sin-1; 50 µM in HBSS) served as the positive control. Fluorescence intensity was measured using a Multimode plate reader (Mithras2, Berthold Technologies) at an excitation wavelength of 485 nm and an emission wavelength of 528 nm.

Likewise 8×10^4 THP-1 cells were seeded per well of a 96-well cell culture plate in 200 µL complete cell culture medium containing 200 nM PMA and allowed to differentiate under standard growth conditions for 72 h. Thereafter cells were washed twice with pre-warmed (37 °C) HBSS and loaded with 50 µM H$_2$DCF-DA in HBSS for 1 h under standard growth conditions. Treatment and measurement conditions were identical to those described for A549 cells above.

2.6.5. Data processing

Blank samples that did not contain cells but were treated exactly the same way were run with each cell-based assay. Values given in the graphs are blank-corrected and subsequently normalized to the untreated control sample. The mean and corresponding standard deviations of at least three independent experiments are given. For each experiment three technical replicates were carried out.

3. Results and Discussion

3.1. Synthesis of flame retardants and analysis

The conventional synthesis of DOPO-PEPA using Atherton-Todd method has already reported in the literature [15] The synthesis of DOPO derivatives containing P-O and P-N bonds are usually performed using Atherton-Todd synthetic method where the P-H bond of DOPO is converted to P-Cl in situ. [6,15] This synthetic method is quite simple and versatile for many amine and alcohol based nucleophiles [26]. Carbon tetrachloride (CCl$_4$) is normally used as a chlorinating agent in this case. However, it is toxic [27] and ozone depleting and banned for industrial applications in Europe. Thus any future industrial exploitation of DOPO-derivatives (P-O, and P-N derivatives) synthesized using CCl$_4$ is not feasible. As an alternative to CCl$_4$ as chlorination agent the use of sulfuryl chloride and trichloro cyanuric chloride (TCCA) as chlorinating agents for P-H bond of DOPO has been reported [14]. Sulfuryl chloride is relatively cheap but it is corrosive and requires special handling and its use in the chlorination reaction produces toxic byproducts like SO$_2$ and HCl which need to be trapped and the waste treated. The use of TCCA can be considered sustainable due to its potential reuse (regeneration of cyanuric acid to TCCA) however its reaction with phosphorus compounds is very exothermic and poses potential explosion hazard in big scale synthesis in industry [14].

Herein, we report the use of N-chlorosuccinimide (NCS) (Scheme 1) as chlorinating agent for converting P-H bond of DOPO to P-Cl. Despite its utilization as a chlorinating agents for hydrocarbons [28—30], to the best of our knowledge, its use in converting P(O)-H bond to P(O)-Cl bond is limited to hydrogen phosphonates [31—33]. The use of NCS as chlorinating agent can be considered sustainable because the major byproduct formed in the chlorination reaction (Scheme 1) is succinimide which can be recovered and reused to regenerate the NCS. This methodology is promising for industrial exploitation as green and effective low-cost synthetic route without non-desirable waste products [34]. It is further noted here; despite our best efforts to replace dichloromethane as solvent with other environment friendly solvents we couldn't improve the yield of the reaction especially in the second stage. Though the chlorinating step can be performed with other solvents such as acetonitrile, toluene, 2- methyl tetrahydrofuran, etc. the subsequent step of reaction with PEPA resulted in complications like poor yields, low solubility of PEPA and formation of many byproducts which were not possible to be removed.

The synthesis of AAM-DOPO via a Michael Addition reaction in toluene and a catalyst (1,8-diazabicyclo[5.4.0]undec-7-ene) is reported by Liu et al. [21]. A solvent and catalyst free synthetic strategy can be considered green. Thus we in this work report a solvent and catalyst free microwave assisted synthesis of AAM-DOPO similar to a method reported in the literature [35]. The synthesis of AAM-DOPO was performed using 2 equivalent of acrylamide to DOPO which resulted in higher yields (67%) as compared to 1:1 (DOPO: acrylamide) molar ratio (39%). Higher amount of acrylamide could ensure more probability of Michael addition compared to other side reactions like self-addition to form polyacrylamide. The temperature of the reaction (120 °C) was chosen so as to ensure melting of acrylamide and DOPO and good mixing. Excess of unreacted acrylamide and possible byproducts could be easily removed by washing with water. The yields reported for other DOPO derivatives using this methodology is higher which may be due to the use of small scale reactions and less reactive alkenes [35]. Unlike the solvent based cleaning procedure in this work only simple water based washing procedure was used to remove the byproducts and starting materials. The synthesis methodologies for both compounds concerning sustainability described in this work were not fully optimized. Detailed work on optimized synthesis methodology is intended for future publications.

Figs. S3 and S4 (Supporting Information) illustrate the thermal data of the FRs. Understanding the thermal behavior of the FRs may help us predict and understand their subsequent processing, thermal and fire behavior of the materials produced from them. As seen from Fig. S3, among all FRs used in this research the lowest melting point is exhibited by AAM-DOPO (~170 °C) followed by DOPO-PEPA (~230 °C) and Aflammit (~250 °C). As these FRs melt under the processing condition of PET and PBT, it is very likely that these additives will have plasticizing effect on the polymers during their thermal processing. Furthermore all additives exhibited relatively high thermal decomposition temperatures (T$_{D\ 5\%}$), greater than 250 °C. The DOPO derivatives had higher thermal stabilities compared to Aflammit PCO 960 i.e. ~300 °C and ~380 °C for AAM-DOPO and DOPO-PEPA respectively. It is likely that DOPO derivatives will be more suitable for processing with PET compared to Aflammit PCO 960. High thermal stability of DOPO-PEPA could offer process stability and possible recyclability of the final material. Aflammit PCO 960 and AAM-DOPO decomposes via one step decomposition process (Fig. S4) without leaving any significant residue at 800 °C. It is likely that these additives volatilize and may be predominantly active in the gas phase compared to DOPO-PEPA which leaves a considerable residue of more than 40% at 800 °C. The PEPA component of DOPO-PEPA is known to work in condensed phase [36,37].

3.2. Thermodynamic compatibility of FRs with polyesters

It is important to ensure a satisfactory thermodynamic affinity between the FRs and the polyesters in order to avoid any severe
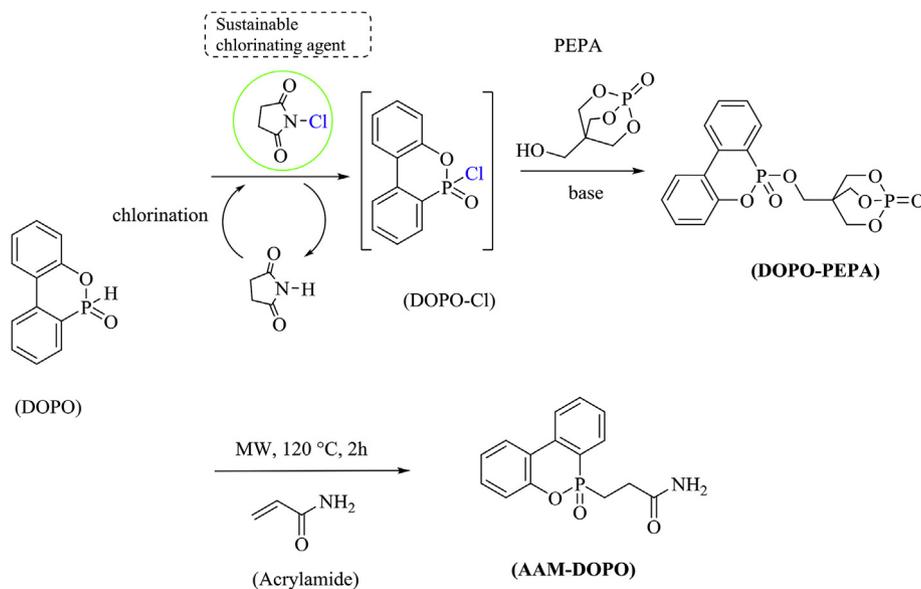
Scheme 1. Green synthesis strategies for DOPO derivatives.

phase separation during their processing. The thermodynamic compatibility of different components in the blends can be elucidated in terms of the classic solubility parameters defined for different components [23]. These parameters can be determined either experimentally or theoretically. Theoretical methods which are often used in literature to determine the solubility parameter of a new molecule include the detailed atomistic simulations of a compilation of molecular configurations [22] and the group contribution method [38,39]. In this work, the solubility parameters of the polyesters were taken from the literature [40—43]. Additionally, atomistic MD simulations were used to calculate the solubility parameters of the FR molecules. The results are summarized in Table 2. DOPO-PEPA has the lowest solubility parameter among all FR additives which is due to its relatively low electrostatic contributions. The lower electrostatic contribution to the total energy of the simulated material (at relatively similar van der Waals contributions) results in a smaller total non-bonded energy to volume ratio which translates to the total cohesive energy density [44,45]. Thus, DOPO-PEPA can be considered the most compatible FR for PET from the thermodynamic point of view, while AAM-DOPO has a poorer miscibility with PET. In PBT blends, Aflammit PCO 960 is the most compatible FR with the matrix, although DOPO-PEPA still shows good compatibility with PBT. One can conclude that DOPO-PEPA and Aflammit PCO 960 both show good compatibilities with the polyesters, whereas the compatibility of AAM-DOPO is relatively poor in both polymers. These theoretical calculations regarding the compatibility of the additives correlate well with the processability data of the additives as described later. It should be noted that an upper-scale mesoscopic perspective on the compatibility of each component with the polymers could be further provided if one utilizes the total solubility parameter data in coarse-grained dissipative particle dynamics simulations [46—48]. Such simulations, however, are not expected to add new findings to the current paper and are thus postponed to a later manuscript.

3.3. Film extrusion

In the course of this work several film extrusion trials were performed, see Table 1 and Table S1. The processing of DOPO-PEPA with both PBT and PET was relatively trouble free with the exception that DOPO-PEPA acted as plasticizer and increased the flowability of the polymer melt, which was compensated by reducing the temperature of the slit die. Aflammit PCO 960, on the other hand, exacerbated processability when co-extruded with PBT, most probably because it did not melt completely at the required processing temperature (~240 °C). However with PET, Aflammit PCO 960 shows relatively good processability. Like DOPO-PEPA, AAM-DOPO also tends to increase the flowability of the polymer melt most probably due to its plasticizing effect. Feeding the additive into the extruder was impeded by gradual decomposition (indicated by a yellowing of the melt) and agglutination of AAM-DOPO, which led to discontinuous processing of the materials. In general, addition of FRs to the polyesters rendered the material prone to stick on the take up calender rolls (Fig. 3) during their processing, which sometimes resulted in an uneven film surface. No attempt to further optimize the film forming process was undertaken as it is beyond the scope of this study. The films were evaluated for their phosphorus content and the data is reported in Table 1. To check homogeneity of the films, phosphorus content was checked at various places along the length and width of the films. The

Table 2
The solubility parameters of FRs (calculated from the MD simulations) and the two polyesters (experimentally and/or theoretically derived by others for PET [40—42] and PBT [43]). For the FRs, the contributions of the van der Waals and electrostatic interactions to the overall solubility parameters are also given separately.

Material	Total solubility parameter $(J/cm^3)^{0.5}$	Van der Waals solubility parameter $(J/cm^3)^{0.5}$	Electrostatic solubility parameter $(J/cm^3)^{0.5}$
AAM-DOPO	22.9	19.6	11.1
DOPO-PEPA	21.0	18.9	8.0
Aflammit PCO 960	21.4	17.8	11.1
PET	19.9—21.9		
PBT	21.1—22.6		

phosphorus content was found to be relatively constant throughout the films and the actual phosphorus content matched well with the predicted content. However, the PBT/AD and PET/AD films had lower actual phosphorus content compared to the theoretical concentration. This may be due to possible process instability we experienced in the film extrusion process as mentioned above in the text.

3.4. Thermal analysis of the films

The TGA and DSC data of polyester films in N_2 environment shown in Figs. S5 and S6 of the Supporting Information are summarized in Table 3. Addition of FR additives to both polyesters has negligible influence on the melting point (estimated from the second DSC cycle) of the polymer. However, the recrystallization point for the PET is influenced by presence of additives. It is likely that the FR additives act as nucleating agent and shift the onset of crystallization to a higher temperature. It is well-known that the crystallization rate of virgin PET is rather low, and can be promoted by additives that act as nucleating agents [49]. Except in case of PET/DP blend, the TGA data clearly shows that addition of FR additives lowers the initial decomposition temperature ($T_{D5\%}$) of the polyesters. Aflammit PCO 960 and AAM-DOPO have the strongest influence in lowering the initial decomposition temperature ($T_{D5\%}$) which correlates well with their lower thermal stability as described earlier. The main stage decomposition of all polyesters remains mostly similar irrespective of addition of any FR additive. Except for the PET/DP blend, the residue for all polyesters at 800 °C remains similar to the blank polyesters. PET/DP shows significantly higher residue at 800 °C which may be due to possible condensed phase action of the PEPA component [36,37]. As discussed earlier, DOPO-PEPA by itself has more than 40% residue at 800 °C and this could increase also the char content of the formulation considering no interaction of FR with the polymer. It is very likely that these additives, particularly Aflammit PCO 960 and AAM-DOPO, act primarily in the gas phase and have negligible influence in the condensed phase.

3.5. Stability of polyester/FR melts

In order to provide a measure of the viscoelasticity of the polyester melts, oscillatory amplitude sweep experiments were carried out and the data is presented in Fig. 4a and b. All polyester formulations exhibit a more dominant viscous behavior than an elastic response under the testing conditions. The PBT samples containing FRs show lower storage and loss moduli than the neat PBT sample indicating an easier overall flowability of the melts with FRs which augments our assumptions about possible plasticizing effect of the additives as described earlier. The PET samples with FRs also show a similar behavior except for the PET

sample containing Aflammit PCO 960. The PET/AF blend shows an increase in the storage modulus at higher strains. However, this increase could be due to changes in the material behavior as a function of time rather than a strain-induced phenomenon. In previous studies, it has been shown that PET melts undergo significant thermal and thermal-oxidative changes [50–53]. These changes are mainly concerned with the chain scission and crosslinking of PET chains at elevated temperatures in the presence and/or absence of oxygen. Considering that a single curve of amplitude sweep is measured in a single run, it can be expected that similar changes influence the results to some extent. In fact, a gradual decay in the melt moduli of all of the samples (except for the PET/AF) is evident prior to the onset of the strain-induced nonlinear deformations region. Such decay is generally ascribed to the degradation behavior of the molten polymer [52]. Consequently, we have investigated the stability of the melt properties of the polyester blends at elevated temperatures in the presence of oxygen and the data is presented in Fig. 4 c,d. According to the results, PBT blends show a typical exponential decay in their viscosity with time, indicating the thermal degradation of the polymer melt. These results support earlier hypothesis that the time-dependent molecular changes at elevated temperatures influence the gradual decay in the oscillatory moduli in the linear region of the amplitude sweep tests. However, the PET and its blends behave somewhat differently. The neat PET sample shows an increase in its viscosity over time as opposed to the decay observed for the neat PBT. This behavior has been observed before and is linked to the competition between chain scission and crosslinking taking place in the melt under either nitrogen or oxygen environments [50,52,53]. It has been argued that oxygen triggers such chemical reactions. Therefore, the stability of the melt is critical and should be considered prior to promoting the materials for commercialization, particularly since the recycling of PET is necessary to obtain a sustainable environmental-friendly production. Indeed, it is important to consider the melt stability on longer time scales to ensure steady and problem free recycling using extrusion. In some cases the extruder blockage is reported for PET melts after a few extrusion cycles due to the crosslinking reactions [53]. Our results show that the incorporation of Aflammit PCO 960 in PET as an additive drastically diminishes its long term melt stability during the processing by either activating new crosslinking reactions, or accelerates the already existing crosslinking reactions. DOPO-PEPA, on the other hand, seems to control the crosslinking behavior of PET chains and promote a typical degradation behavior over time. To see how the crosslinking affects the samples, we conducted DSC tests in repeating cycles from 20 °C to 300 °C and back to 20 °C again (the results of these experiments are given in Supporting Information Table S2). According to our findings, the crystallinity of the PET/AF blend is dramatically reduced with each heating-

Table 3
Thermal data of the polyester films.

Sample name	$T_{D5\%}/N_2$ [°C]	TD-main /N_2 [°C]	Residue at 800 °C /N_2 [w%]	Melting Point [°C]	Recrystallization Point [°C]
PBT	363	393	4.86	224	194
PBT/AF	353	391	0.51	223	195
PBT/DP	356	391	2.56	222	193
PBT/AD	351	393	2.38	222	194
PET	388	432	7.22	253	185
PET/AF	380	425	8.08	247	200
PET/DP	388	429	16.32	252	189
PET/AD	373	429	5.59	254	208
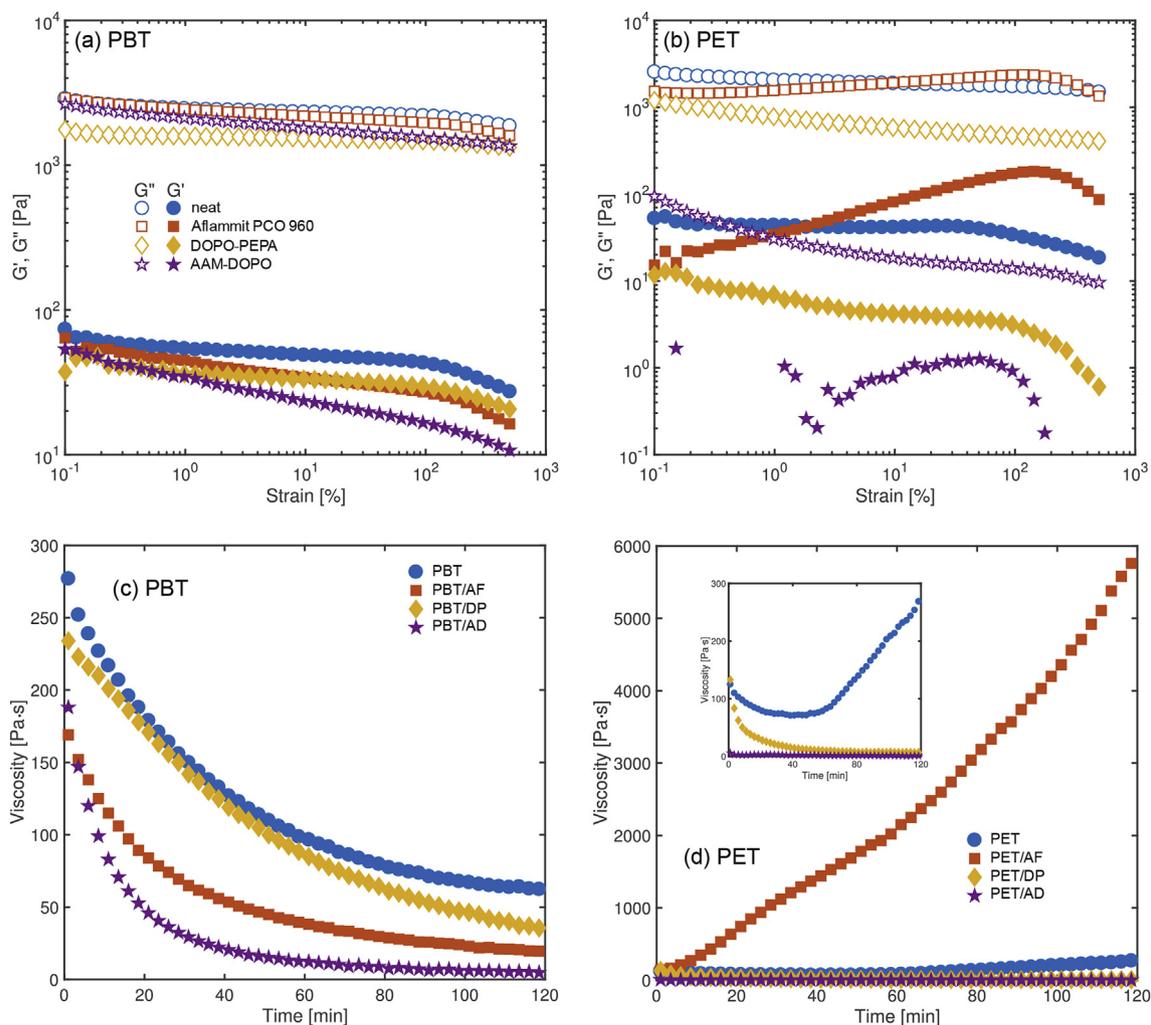
Fig. 4. Storage G′ and loss G″ moduli in oscillatory amplitude sweep experiments of (a) PBT and (b) PET blends with different FRs. The legends of part b are the same as those in part a. Oscillatory time sweep experiments of (c) PBT and (d) PET blends with different FRs. The inset in part d shows the data for PET samples in greater details. In the beginning of the time sweeps tests, the viscosity of PBT (at 250 °C) and PET (at 290 °C) melts are ~277 and ~125 Pa s, respectively.

cooling cycle whereas the crystallinity does not alter to the same extent for PET/DP. One can attribute such a significant change in the crystallization of the polymer chains to the crosslinking of the polymer chains, which prevents crystallization [54]. As for the PET/AD sample, the melt viscosity drops so strongly by the addition of the FR that it can considerably complicate its processability in the extruder under normal processing conditions. This situation is, however, less prominent in the PBT/AD blend which is indeed processed at a considerably lower temperature (235 °C in PBT vs 265 °C in PET). The results show that DOPO-PEPA develops more stable melts over longer time scales with both polymers, and exhibit typical rheological characteristics, thus, promoting their use in further recycling processes. DOPO-PEPA can facilitate the processability of PET and PBT while providing useful FR property to the final product, thus, resulting in easy-to-process functional materials. Finally, it should be noted that the systematic difference in rheological behavior of PET/AF and PBT/AF melts over time could be ascribed to their different experimental temperatures. PBT/AF is tested at 250 °C whereas PET/AF at 290 °C. The thermo-oxidative crosslinking is temperature-dependent and the lower testing temperature of PBT/AF may not be enough to initiate the crosslinking reactions and their propagation (kinetics must be fast) [50,52,53].

3.6. Small scale fire tests

Polyester films need to be flame retardant in certain applications such as electronics, transportation, construction and label industries. We have thus preliminary evaluation of the FR performance of the films via small scale fire tests. Table 4 summarizes the fire results of the films. In the vertical fire test (BKZ-VB) the

Table 4
Summary of small scale fire tests.

Sample Name	BKZ-VB[a] Test			LOI % ±0.2
	After Flame (sec) ±1	Burn Length (cm) ±0.1	Melt Drips	
PBT	42	15	Many	24.4
PBT/AF	6	8	NO	27.6
PBT/DP	2	6	Few	28.5
PBT/AD	3	6.9	Few	29.7
PET	53	15	Many	24.6
PET/AF	4	7	No	35.3
PET/DP	0	6	No	35.2
PET/AD	0	7	No	43.2

[a] Swiss standard vertical fire test.

blank polyester (PBT and PET) both burned through completely leaving no residue. Addition of FR additive reduced the burn length for the films with all additives performing similarly in both polyesters. However, the polyester/DOPO blends had lower after flame times compared to Polyester/Aflammit PCO 960 blends which may be due to gas flame inhibition of DOPO. In case of PET/DP and PET/AD, the films stopped burning before the burner was removed from the specimen clearly demonstrating their FR efficacy. Flame retardant PBT films on an average burned longer compared the PET films, which may be due to higher aliphatic content compared to PET. In addition, the polyester films with FRs exhibited no or small amount of drips compared to the blank polyester films. Flammable drips are critical in causing bodily injuries and propagation of fire.

The limiting oxygen index of polyesters/FR blend was significantly higher than the blank polyesters. The flame retardant PET films exhibited higher LOI values compared to the PBT samples. In addition the PET/AM and PBT/AM films exhibited the highest LOI value of 43% and 29.7% respectively. It is likely that AAM-DOPO works primary in the gas phase. Flame retardants working in the gas phase usually have greater influence on increasing the LOI of the material. In addition, polyesters with higher C:H ratio or higher aromatic content usually exhibit better flame retardancy [55]. A LOI value more than 28% indicates self-extinguishing behavior of the blends. Thus it is clear that small addition of FR greatly improves the flame retardant behavior of the polyesters studied in this work.

3.7. Thermal decomposition pathways and mode of action of FR additives

To further understand the possible mode of action of the FR additives in condensed phase we have carried out investigations of char residue formed in TGA experiments. The elemental analysis(C, O, P) of chars obtained in the TGA experiments are summarized in table S 3. It is noted here that about 50 mg of films were taken for TGA experiments (N_2 environment) and the residue at 800 °C was removed and homogenized before EDX experiment. As expected no phosphorus (P) can be observed for blank PBT and PET samples. However, for all FR containing films,

Note: Structures depicted in grey are species identified in DIP-MS
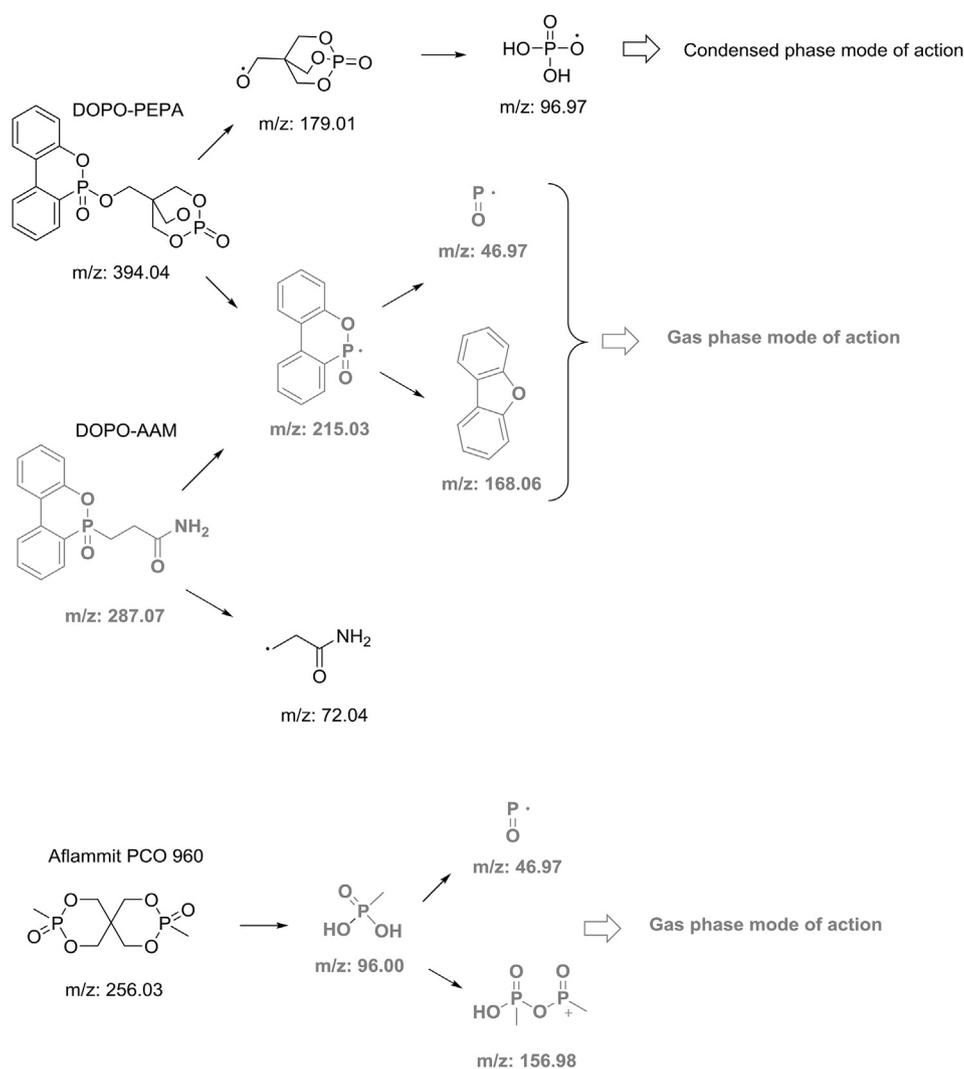
Scheme 2. Proposed thermal decomposition pathways for FR additives based on DIP-MS analysis.

different levels of P was observed in their respective chars. For each polymer (PET or PBT) containing DOPO-PEPA, higher %P in char was recorded followed by AAM-DOPO and Aflammit PCO 960. The presence of phosphorus in the char clearly indicates certain level of condensed phase activity for the three FR additives. Slight improvement in char content for PET (Table 3) and higher % P content in the char for DOPO-PEPA samples clearly indicates higher condensed phase activity of DOPO-PEPA compared to the other FR additives.

As there was only a limited char (Table 3) formed for the polyester films, it is very likely that the FR additives investigated in this research primarily work in the gas phase. Thus evolved gas analysis using DIP-MS was performed to evaluate various volatile phosphorus species formed during the thermal decomposition of the films. Fig. S7 shows the total ion chromatogram (TIC) for various PBT (A) and PET (B) formulations. Virgin PET and PBT decompose in one step at temperatures above 400 °C. This is verified by presence of a single peak after 400 °C in the TIC for PBT and PET (Fig. S7 A and B). However, all FR polyester formulations showed two stage decomposition, where an additional peak at an earlier temperature (150—300 °C) was also observed. For AAM-DOPO and Aflammit PCO 960/polyester formulations this earlier peak was centered at around 270 °C whereas for DOPO-PEPA/polyester formulations the peak is centered at 290 °C. Extracted ion chromatogram of all PBT and PET formulations are further shown in Figs. S8 and S9 respectively. For simplicity we have only analyzed the first stage (150—300 °C) volatile decomposition products of the polyester formulations as the ions at this stage only corresponds to the respective FR additives. At later stage above 300 °C things become complicated due to the formation vast numbers of decomposition products from the polymer matrix. For DOPO-PEPA and AAM-DOPO

formulations species corresponding to m/z 47, 168 and 216 were observed which represents $PO^{\bullet}$, dibenzofuran and DOPO respectively. Earlier studies have also identified the same species for DOPO derivatives [14,56]. In addition, for AAM-DOPO formulations we observed species corresponding m/z 287 and was identified as AAM-DOPO itself. In case of Aflammit PCO 960 formulations, species corresponding to m/z 47, 97 and 157 were observed which represent PO, methyl phosphonic acid and a pyrophosphate respectively. Similar species have also been identified for Aflammit PCO 960 in another study [57]. Based on these observations we have proposed the simplistic decomposition pathways for the FR additives in Scheme 2 and their possible mode of action.

Thus DOPO-PEPA and AAM-DOPO decomposes to produce DOPO radical in the gas phase. This pathway is supported by the presence of species corresponding to m/z 168 (dibenzofuran) and 47 ($PO^{\bullet}$) in the extracted ion chromatograms. In addition the PEPA unit of DOPO-PEPA could remain in the condensed phase to produce phosphoric acids which can be responsible for condensed phase activity. Increased char formation for PET/DP formulations as observed in TGA corroborates this hypothesis. Meanwhile, Aflammit PCO 960 decomposes to form methyl phosphonic and acidic pyrophosphate (Scheme 2) in the gas phase which ultimately produces $PO^{\bullet}$ corresponding to m/z 47. It is well known that $PO^{\bullet}$ is the active species responsible for flame inhibition [25,58].

3.8. Preliminary toxicity data of FR additives

In order to assure sustainable development, production and use of new materials (i.e. FR additives) safety assessment of these new materials is indispensable. As comprehensive toxicological
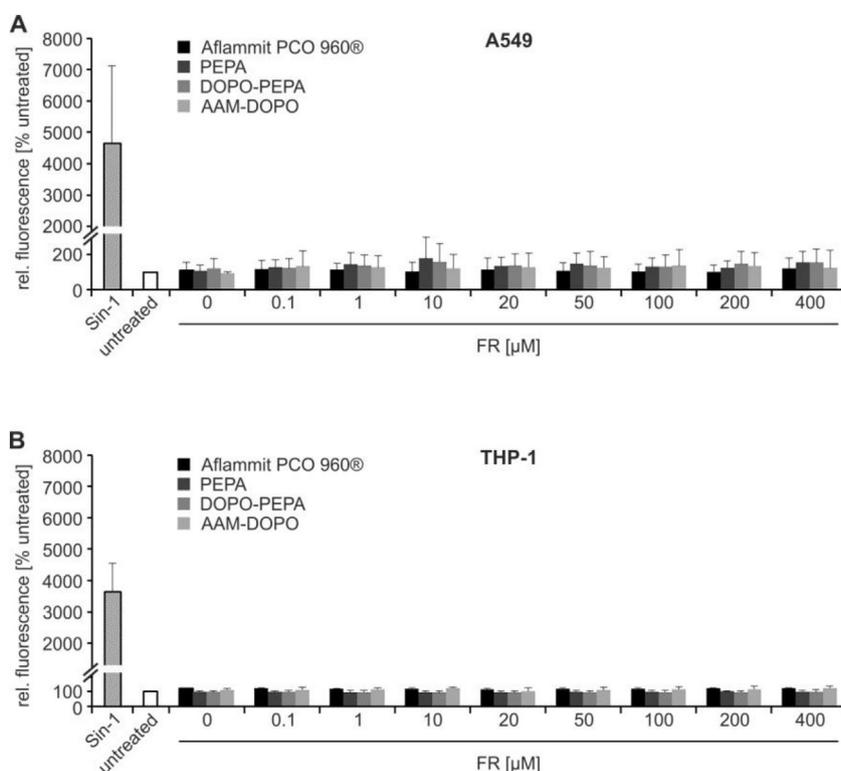
Fig. 5. Analysis of ROS overproduction in A549 and THP-1 cells in the presence of FR additives. (ROS formation was measured in (A) A549 cells as well as (B) differentiated THP-1 macrophages. None of the flame retardants analyzed induced elevation of ROS levels at concentrations up to 400 μM and 2 h of incubation. Sin-1 (50 μM) served as the positive control. Values are normalized to untreated control samples and represent the mean and corresponding standard deviations of three independent experiments.).
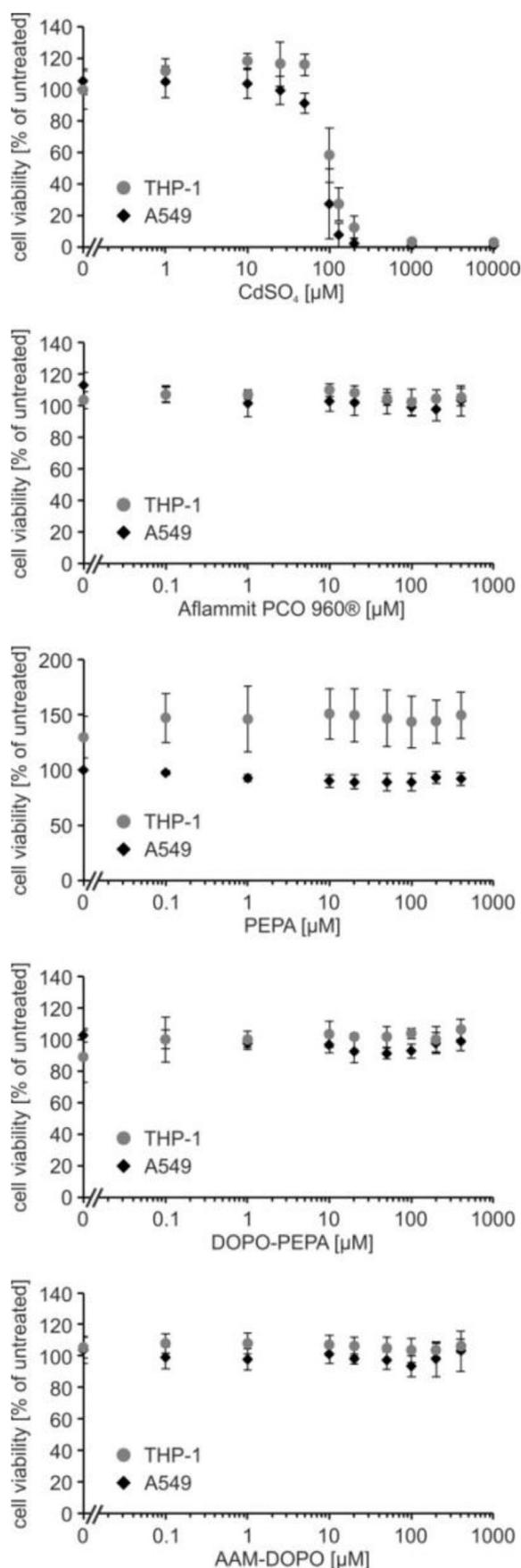
evaluations *in vivo* (in animals) is very time consuming and costly these can hardly be performed side-by-side with the lab-scale development of new materials. Nevertheless first safety indicators are urgently needed to choose from a set of promising additives not only the most efficient one in terms of flame retardancy and processabilty but also the presumably safest one for production and application.

Therefore we made use of a well-established *in vitro* platform for toxicity evaluation of the new additives that allows studying potential adverse effects on cell viability in due time and following the ideas ISO and OECD guidelines. This platform has been successfully applied in a previous study as one of several *in vitro* methods to determine FR induced acute cytotoxicity [18]. According to the so-called ROS paradigm the overproduction of reactive oxygen species (ROS) by cultured cells is one of the first indicators of cellular stress reactions. While efficient anti-oxidant defense mechanisms can circumvent subsequent cell injury, persistent ROS overload can seriously damage biomolecules (such as lipids, nucleic acids and proteins), induce inflammation and finally lead to cell death [59—65]. In a fast screening approach we assessed the first stressor (overproduction of ROS) as well as the last, most deleterious step of the cascade (cell death) in response to FR additives in two model cell lines: the human lung epithelial cell line A549 and macrophages derived from the monocytic cell line THP-1 (Fig. 5).

FR concentrations up to 400 μM were applied to A549 lung epithelial cells as well as THP-1 derived macrophages. These resemble worst case but still realistic exposure concentrations [18] and are comparable to available literature on flame retardant toxicity studies *in vitro* [66,67] allowing for direct comparison of the results. In this concentration range, none of the FRs induced the elevation of ROS above background levels of untreated control samples (Fig. 5) for both cell types. In contrast treatment with 50 μM of the positive control Sin-1 resulted in a 46- and 36-fold increase in fluorescence signal intensity after 2 h of A549 and THP-1 treatment respectively.

This particular assay is able to assess the first burst release of ROS within the first minutes and hours of treatment. Even though cells were not impaired by any of the FRs within this timeframe, later effects on cell viability cannot be excluded so far. Therefore potential adverse effects on cell viability were determined after 3, 24 and 48 h of treatment by measuring the reduction of the tetrazolium compound MTS. Incubation of A549 as well as differentiated THP-1 cells with increasing concentrations of the positive control Cadmiumsulfate ($CdSO_4$) resulted in dose-dependent cell death (Fig. 6). In contrast none of the FRs had any influence on A549 and THP-1 cell viability at concentrations up to 400 μM and up to 48 h of incubation (Fig. 6 and Fig. S10 of the Supporting Information for 3 and 24 h reading points).

Taken together our results indicate no acute cytotoxic potential for all FRs analyzed in two different cell types and under the experimental conditions chosen. It should however be noted that subtoxic effects such as inflammatory reactions could still have been overlooked in this initial screening. Further in-depth analyses are needed to fully elucidate potential health risks especially in *in vivo* situations. Furthermore, ecotoxicological aspects as described for a different DOPO derivative (DOPO-HQ [20]) are also pending before commercializing new products. This however is beyond the scope of the present study.

Fig. 6. Analysis of cell viability in A549 and THP-1 cells in the presence of FR additives. (Cell viability is not influenced by any of the flame retardants up to a concentration of 400 μM and 48 h of incubation. A549 cells as well as THP-1 macrophages were treated for 48 h with the indicated increasing concentrations of flame retardants. Cell viability was measured using the MTS assay. Values are normalized to untreated control samples and represent the mean and corresponding standard deviations of three independent experiments.)

4. Conclusions

In this work comprehensive strategies *i.e.* green synthesis methodology, detailed material characterization and first toxicity evaluation of the FR additives as a way to develop fire safe sustainable polyesters were presented with an eventual goal for future commercialization. Both DOPO-based additives (DOPO-PEPA and AAM-DOPO) were synthesized using green chemistry principles and compared with the commercial FR additive Aflammit PCO 960. The DOPO derivatives could be processed with high temperature polyesters like PET and PBT due to their high thermal stability. Theoretical data obtained via atomistic simulations and experimental data obtained via rheological measurements indicate that DOPO-PEPA offers the most steady and sustainable melt processing conditions with polyesters compared to the other two FR additives. The polyester films containing all FR additives passed the vertical fire tests and exhibited higher LOI values compared to the virgin polyester films. TGA data and elemental analysis of char obtained for FR formulations indicates possible limited condensed phase activity of the FR additives. We could identify phosphorus based volatile species in the evolved gas analysis performed using DIP-MS. Such phosphorus species could be responsible for the gas phase flame inhibition and thus improving the flame retardancy of the polymer in this study. Based on the DIP-MS data we have also proposed simplified decomposition pathways of the FR additives. In case of DOPO derivatives DOPO radical was clearly observed as one of the volatile species. Methyl phosphonic acid was observed as the primary volatile spices in case of Aflammit PCO 960. All FR additives were shown to be non-toxic in the *in vitro* assays and conditions chosen. Thus in this study, detailed multi-dimensional analyses of these relatively new FR molecules were provided with focus on the green chemistry principles at the synthesis level, the thermooxidative stability at the processing stage, fire and environmental safety during the product consumption, and the prospect of sustainability at the recycling stage.

Author contributions

The manuscript was written through contributions of all authors. All authors have given approval to the final version of the manuscript.

Funding sources

Acknowledgment

Appendix A. Supplementary data

Supplementary data related to this article can be found at https://doi.org/10.1016/j.polymdegradstab.2018.07.006.

References

[1] A. DeVierno Kreuder, T. House-Knight, J. Whitford, E. Ponnusamy, P. Miller, N. Jesse, et al., A method for assessing greener alternatives between chemical products following the 12 principles of green chemistry, ACS Sustain. Chem. Eng. 5 (2017) 2927—2935.

[2] P.A. Wäger, M. Schluep, E. Müller, R. Gloor, RoHS regulated substances in mixed plastics from waste electrical and electronic equipment, Environ. Sci. Technol. 46 (2012) 628—635.

[3] F. Rahman, K.H. Langford, M.D. Scrimshaw, J.N. Lester, Polybrominated diphenyl ether (PBDE) flame retardants, Sci. Total Environ. 275 (2001) 1—17.

[4] M. Rakotomalala, S. Wagner, M. Döring, Recent developments in halogen free flame retardants for epoxy resins for electrical and electronic applications, Materials 3 (2010) 4300.

[5] S.-Y. Lu, I. Hamerton, Recent developments in the chemistry of halogen-free flame retardant polymers, Prog. Polym. Sci. 27 (2002) 1661—1712.

[6] K.A. Salmeia, S. Gaan, An overview of some recent advances in DOPO-derivatives: chemistry and flame retardant applications, Polym. Degrad. Stabil. 113 (2015) 119—134.

[7] S. Wendels, T. Chavez, M. Bonnet, K. Salmeia, S. Gaan, Recent developments in organophosphorus flame retardants containing P-C bond and their applications, Materials 10 (2017) 784.

[8] A. Farhat, D. Crump, S. Chiu, K.L. Williams, R.J. Letcher, L.T. Gauthier, et al., In ovo effects of two organophosphate flame retardants-TCPP and TDCPP-on pipping success, development, mRNA expression, and thyroid hormone levels in chicken embryos, Toxicol. Sci. 134 (2013) 92—102.

[9] K.L. Hill, T. Hamers, J.H. Kamstra, W.G. Willmore, R.J. Letcher, Organophosphate triesters and selected metabolites enhance binding of thyroxine to human transthyretin in vitro, Toxicol. Lett. 285 (2018) 87—93.

[10] C. Huang, N. Li, S. Yuan, X. Ji, M. Ma, K. Rao, et al., Aryl- and alkyl-phosphorus-containing flame retardants induced mitochondrial impairment and cell death in Chinese hamster ovary (CHO-k1) cells, Environ. Pollut. 230 (2017) 775—786.

[11] P.J. Morris, D. Medina-Cleghorn, A. Heslin, S.M. King, J. Orr, M.M. Mulvihill, et al., Organophosphorus flame retardants inhibit specific liver carboxylesterases and cause Serum hypertriglyceridemia, ACS Chem. Biol. 9 (2014) 1097—1103.

[12] I. van der Veen, J. de Boer, Phosphorus flame retardants: properties, production, environmental occurrence, toxicity and analysis, Chemosphere 88 (2012) 1119—1153.

[13] P. Jiang, X. Gu, S. Zhang, S. Wu, Q. Zhao, Z. Hu, Synthesis, characterization, and utilization of a novel phosphorus/nitrogen-containing flame retardant, Ind. Eng. Chem. Res. 54 (2015) 2974—2982.

[14] N.M. Neisius, M. Lutz, D. Rentsch, P. Hemberger, S. Gaan, Synthesis of DOPO-based phosphonamidates and their thermal properties, Ind. Eng. Chem. Res. 53 (2014) 2889—2896.

[15] T. Stelzig, L. Bommer, S. Gaan, A. Buczko, Dopo-based hybrid flame retardants, in: Empa Eidgenoessische Materialpruefungs- und Forschungsanstalt, Switz., 2015, 22pp.; Chemical Indexing Equivalent to 163:474006 (EP).

[16] S. Wagner, M. Rakotomalala, Y. Bykov, O. Walter, M. Döring, Synthesis of new organophosphorus compounds using the atherton—todd reaction as a versatile tool, Heteroat. Chem. 23 (2012) 216—222.

[17] S.L. Waaijers, J. Hartmann, A.M. Soeter, R. Helmus, S.A.E. Kools, P. de Voogt, et al., Toxicity of new generation flame retardants to Daphnia magna, Sci. Total Environ. 463—464 (2013) 1042—1048.

[18] C. Hirsch, B. Striegl, S. Mathes, C. Adlhart, M. Edelmann, E. Bono, et al., Multiparameter toxicity assessment of novel DOPO-derived organophosphorus flame retardants, Arch. Toxicol. 91 (2017) 407—425.

[19] M.B. Gustavsson, A. Hellohf, T. Backhaus, Evaluating the environmental hazard of industrial chemicals from data collected during the REACH registration process, Sci. Total Environ. 586 (2017) 658—665.

[20] M. Liu, H. Yin, X. Chen, J. Yang, Y. Liang, J. Zhang, et al., Preliminary ecotoxicity hazard evaluation of DOPO-HQ as a potential alternative to halogenated flame retardants, Chemosphere 193 (2018) 126—133.

[21] X. Liu, K.A. Salmeia, D. Rentsch, J. Hao, S. Gaan, Thermal decomposition and flammability of rigid PU foams containing some DOPO derivatives and other phosphorus compounds, J. Anal. Appl. Pyrol. 124 (2017) 219—229.

[22] M. Belmares, M. Blanco, W.A. Goddard, R.B. Ross, G. Caldwell, S.H. Chou, et al., Hildebrand and Hansen solubility parameters from Molecular Dynamics with applications to electronic nose polymer sensors, J. Comput. Chem. 25 (2004) 1814—1826.

[23] C.M. Hansen, Hansen solubility Parameters: a User's Handbook, CRC press, 2007.

[24] I. Accelrys, BIOVIA Materials Studio, 2017.

[25] S. Liang, M. Neisius, H. Mispreuve, R. Naescher, S. Gaan, Flame retardancy and thermal decomposition of flexible polyurethane foams: structural influence of organophosphorus compounds, Polym. Degrad. Stabil. 97 (2012) 2428—2440.

[26] S.S. Le Corre, M. Berchel, H. Couthon-Gourves, J.-P. Haelters, P.-A. Jaffres, Atherton-Todd reaction: mechanism, scope and applications, Beilstein J. Org. Chem. 10 (2014) 1166—1196, 31 pp.

[27] L.W.D. Weber, M. Boll, A. Stampfl, Hepatotoxicity and mechanism of action of haloalkanes: carbon tetrachloride as a toxicological model, Crit. Rev. Toxicol. 33 (2003) 105—136.

[28] N. Halland, A. Braunton, S. Bachmann, M. Marigo, K.A. Jorgensen, Direct organocatalytic asymmetric α-chlorination of aldehydes, J. Am. Chem. Soc. 126 (2004) 4790—4791.

[29] Y.-C. Liu, C.-F. Lee, N-Chlorosuccinimide-promoted synthesis of thiophosphates from thiols and phosphonates under mild conditions, Green

Chem. 16 (2014) 357–364.

[30] R.-J. Tang, T. Milcent, B. Crousse, Regioselective halogenation of arenes and heterocycles in hexafluoroisopropanol, J. Org. Chem. 83 (2018) 930–938.

[31] G.W. Kenner, A.R. Todd, F.J. Weymouth, Nucleotides. XVII. N-Chloroamides as reagents for the chlorination of diesters of phosphorous acid. New synthesis of uridine-5'-pyrophosphate, J. Chem. Soc. (1952) 3675–3681.

[32] H. Goldwhite, B.C. Saunders, Esters containing phosphorus. XII. Esters of phosphofluoridic acid, J. Chem. Soc. (1955) 2040–2041.

[33] Z. Skrzypczynski, J. Michalski, Stereoselective synthesis and stereochemistry of optically active tert-butylphenylphosphine sulfide, J. Org. Chem. 53 (1988) 4549–4551.

[34] K. Salmeia, F. Flaig, D. Rentsch, S. Gaan, One-pot synthesis of P(O)-N containing compounds using N-Chlorosuccinimide and their influence in thermal decomposition of PU foams, Polymers 10 (2018) 740.

[35] R.A. Stockland, R.I. Taylor, L.E. Thompson, P.B. Patel, Microwave-assisted regioselective addition of P(O)–H bonds to alkenes without added solvent or catalyst, Org. Lett. 7 (2005) 851–853.

[36] W. Zhang, X. He, T. Song, Q. Jiao, R. Yang, The influence of the phosphorus-based flame retardant on the flame retardancy of the epoxy resins, Polym. Degrad. Stabil. 109 (2014) 209–217.

[37] D. Hoang, J. Kim, Flame-retarding behaviors of novel spirocyclic organo-phosphorus compounds based on pentaerythritol, Macromol. Res. 23 (2015) 579–591.

[38] M.P. Fernández-Ronco, B. Gradzik, A. Gooneie, R. Hufenus, M. El Fray, Tuning poly(3-hydroxybutyrate) (P3HB) properties by tailored segmented bio-copolymers, ACS Sustain. Chem. Eng. 5 (2017) 11060–11068.

[39] E. Stefanis, C. Panayiotou, Prediction of hansen solubility parameters with a new group-contribution method, Int. J. Thermophys. 29 (2008) 568–585.

[40] Y. Fu, L. Liao, L. Yang, Y. Lan, L. Mei, Y. Liu, et al., Molecular dynamics and dissipative particle dynamics simulations for prediction of miscibility in polyethylene terephthalate/polylactide blends, Mol. Simulat. 39 (2013) 415–422.

[41] D. Karst, Y. Yang, Using the solubility parameter to explain disperse dye sorption on polylactide, J. Appl. Polym. Sci. 96 (2005) 416–422.

[42] Z. Rigbi, Prediction of swelling of polymers in 2 and 3 component solvent mixtures, Polymer 19 (1978) 1229–1232.

[43] E. Fekete, B. Pukánszky, Z. Peredy, Mutual correlations between parameters characterizing the miscibility, structure and mechanical properties of polymer blends, Angew. Makromol. Chem. 199 (1992) 87–101.

[44] P. Choi, T.A. Kavassalis, A. Rudin, Estimation of the three-dimensional solu-bility parameters of alkyl phenol ethoxylates using molecular dynamics, J. Colloid Interface Sci. 150 (1992) 386–393.

[45] K. Lee, H.J. Lim, S.J. Yang, Y.S. Kim, C.R. Park, Determination of solubility pa-rameters of single-walled and double-walled carbon nanotubes using a finite-length model, RSC Adv. 3 (2013) 4814–4820.

[46] A. Gooneie, C. Holzer, Reinforced local heterogeneities in interfacial tension distribution in polymer blends by incorporating carbon nanotubes, Polymer 125 (2017) 90–101.

[47] A. Gooneie, J. Sapkota, A. Shirole, C. Holzer, Length controlled kinetics of self-assembly of bidisperse nanotubes/nanorods in polymers, Polymer 118 (2017) 236–248.

[48] A. Gooneie, S. Schuschnigg, C. Holzer, A review of multiscale computational methods in polymeric materials, Polymers 9 (2017) 16.

[49] X.L. Jiang, S.J. Luo, K. Sun, X.D. Chen, Effect of nucleating agents on crystalli-zation kinetics of PET, Express Polym. Lett. 1 (2007) 245–251.

[50] R. Assadi, X. Colin, J. Verdu, Irreversible structural changes during PET recy-cling by extrusion, Polymer 45 (2004) 4403–4412.

[51] J.D. Badía, F. Vilaplana, S. Karlsson, A. Ribes-Greus, Thermal analysis as a quality tool for assessing the influence of thermo-mechanical degradation on recycled poly(ethylene terephthalate), Polym. Test. 28 (2009) 169–175.

[52] M. Kruse, M.H. Wagner, Time-resolved rheometry of poly(ethylene tere-phthalate) during thermal and thermo-oxidative degradation, Rheol. Acta 55 (2016) 789–800.

[53] L.K. Nait-Ali, X. Colin, A. Bergeret, Kinetic analysis and modelling of PET macromolecular changes during its mechanical recycling by extrusion, Polym. Degrad. Stabil. 96 (2011) 236–246.

[54] Y. Zhang, C. Wang, H. Du, X. Li, D. Mi, X. Zhang, et al., Promoting crystallization of polylactide by the formation of crosslinking bundles, Mater. Lett. 117 (2014) 171–174.

[55] T. Deans, D.A. Schiraldi, Flammability of polyesters, Polymer 55 (2014) 2825–2830.

[56] I. Butnaru, M. Fernández-Ronco, J. Czech-Polak, M. Heneczkowski, M. Bruma, S. Gaan, Effect of meltable triazine-DOPO additive on rheological, mechanical, and flammability properties of PA6, Polymers 7 (2015) 1469.

[57] H. Saeidian, M. Babri, Z. Mirjafary, M.T. Naseri, M. Sarabadani, D. Ashrafi, et al., Fragmentation mechanisms in mass spectrometry of Chemical Weapons Convention related spiro alkylphosphonates and alkyldioxaphosphinane ox-ides, Int. J. Mass Spectrom. 369 (2014) 59–70.

[58] L. Shuyu, H. Patrick, N.N. Matthias, B. Andras, G. Hansjörg, L.-G. Joelle, et al., Elucidating the thermal decomposition of dimethyl methylphosphonate by vacuum ultraviolet (VUV) photoionization: pathways to the PO radical, a key species in flame-retardant mechanisms, Chem. Eur J. 21 (2015) 1073–1080.

[59] K. Donaldson, V. Stone, C.L. Tran, W. Kreyling, P.J. Borm, Nanotoxicology, Occup. Environ. Med. 61 (2004) 727–728.

[60] H.J. Johnston, G.R. Hutchison, F.M. Christensen, S. Peters, S. Hankin, K. Aschberger, et al., A critical review of the biological mechanisms underlying the in vivo and in vitro toxicity of carbon nanotubes: the contribution of physico-chemical characteristics, Nanotoxicology 4 (2010) 207–246.

[61] L.K. Limbach, P. Wick, P. Manser, R.N. Grass, A. Bruinink, W.J. Stark, Exposure of engineered nanoparticles to human lung epithelial cells: influence of chemical composition and catalytic activity on oxidative stress, Environ. Sci. Technol. 41 (2007) 4158–4163.

[62] A. Nel, T. Xia, L. Madler, N. Li, Toxic potential of materials at the nanolevel, Science 311 (2006) 622–627.

[63] M. Roesslein, C. Hirsch, J.P. Kaiser, H.F. Krug, P. Wick, Comparability of in vitro tests for bioactive nanoparticles: a common assay to detect reactive oxygen species as an example, Int. J. Mol. Sci. 14 (2013) 24320–24337.

[64] R.P. Schins, A.M. Knaapen, Genotoxicity of poorly soluble particles, Inhal. Toxicol. 19 (Suppl 1) (2007) 189–198.

[65] H. Wiseman, B. Halliwell, Damage to DNA by reactive oxygen and nitrogen species: role in inflammatory disease and progression to cancer, Biochem. J. 313 (1996) 17–29.

[66] H.S. Hendriks, M. Meijer, M. Muilwijk, M. van den Berg, R.H.S. Westerink, A comparison of the in vitro cyto- and neurotoxicity of brominated and halogen-free flame retardants: prioritization in search for safe(r) alternatives, Arch. Toxicol. 88 (2014) 857–869.

[67] N. Ta, C.N. Li, Y.J. Fang, H.L. Liu, B.C. Lin, H. Jin, et al., Toxicity of TDCPP and TCEP on PC12 cell: changes in CAMKII, GAP43, tubulin and NF-H gene and protein levels, Toxicol. Lett. 227 (2014) 164–171.